Electron correlation effects on the dielectric function of liquid metals

P. Giura, R. Angelini, C. Burns, G. Monaco, F. Sette

▶ **To cite this version:**

HAL Id: hal-00000736
https://hal.archives-ouvertes.fr/hal-00000736v2

Submitted on 22 Oct 2003

Electron correlation effects on the dielectric function of liquid metals

P. Giura[1], R. Angelini[1], C. A. Burns[2], G. Monaco[1] and F. Sette[1].

[1] *European Synchrotron Radiation Facility. B.P. 220 F-38043 Grenoble, Cedex France.*
[2] *Department of Physics, Western Michigan University, Kalamazoo, Michigan 49008*

(Dated: October 22, 2003)

The acoustic excitations of the expanded metal solutions Li-NH$_3$ have been measured by inelastic X-ray scattering as a function of the electron density by changing the Li concentration. The dielectric functions of these model metals with very low electron density have been derived from the high frequency sound velocity using the one component plasma approach corrected for screening. Their values, when combined with those from other metals, suggest that the electron correlation induced departure of the dielectric function from the random phase approximation follows a universal behavior whose main parameter is the electron density.

The study of the dynamical properties of interacting electrons is an important topic in solid state physics as shown by the great interest devoted to the understanding of phenomena as superconductivity and giant magnetoresistance. One way to obtain information on the dielectric response of a system of interacting electrons is to study the acoustic excitations of liquid metals, since the speed of sound in these systems is related to the screening action of the electrons on the ionic motion [1]. In fact, in a simple Jellium model with the electrons screening the Coulomb forces between the ions, the speed of sound, c, can be expressed as:

$$c = \frac{\Omega_{pi}}{Q\sqrt{\epsilon(Q)}}. \qquad (1)$$

Here Q is the wave number, $\epsilon(Q)$ is the total dielectric function and Ω_{pi} is the ionic plasma frequency given by: $\Omega_{pi}^2 = (4\pi n_i(Ze)^2)/M$, where M, Ze and n_i are the mass, the charge and the number density of the ions, respectively. In this relation all the details of the electron dynamics are hidden in the dielectric function, $\epsilon(Q)$, that is purely electronic only if the ions contribution can be neglected - this is the case at high frequencies and Q-transfers, where the atomic response of the liquid is totally elastic and one measures the *infinite*-frequency value of the sound velocity, c. The strength of Eq. 1 is to provide a direct link between an electronic property as $\epsilon(Q)$ and a ionic one as c. Therefore, the measurements of c offers the opportunity to check experimentally the validity of theoretical approaches for $\epsilon(Q)$ as, for example, the Random Phase Approximation (RPA), where [1]:

$$\epsilon_{RPA}(Q) = 1 + \frac{4m^2e^2v_F}{\pi\hbar^3Q^2} = 1 + \frac{Q_{RPA}^2}{Q^2}. \qquad (2)$$

Here, m is the electron mass, v_F the Fermi velocity and Q_{RPA} is a measure of the inverse distance over which the self-consistent electric potential associated with the ions penetrates into the electron gas. This approximation is exact in the limit of high electron density, or $r_s\rightarrow 0$. The parameter $r_s = [3/(4\pi n_e)]^{1/3}a_0^{-1}$, with a_0 the Bohr radius and n_e the electron number density, is the ratio between the Coulomb and the kinetic energies of the electrons. The $r_s\rightarrow 0$ limit corresponds, therefore, to the weak coupling limit. As a matter of fact, the RPA works well in metals with a low value of r_s and with no unfilled d or f shells, as shown in the case of Hg and Pb where r_s is ≈ 3 [2]. In metals with higher values of r_s the RPA clearly fails as recently reported for the case of the Li-NH$_3$ solution at the limit of solubility for which r_s is ≈ 7 [3, 4, 5] and for heavy alkali metals [6]. It is believed that the failure of the RPA at large r_s is mainly due to electronic correlation effects. In this context the Li-NH$_3$ solutions provide an interesting model system to investigate the departure of the $\epsilon(Q)$ from the RPA predictions as a function of the electron density - here the r_s value can be widely varied by changing the Li concentration from the saturated solution value r_s=7.4 to the metal-insulator transition value ≈ 12.

In this Letter we report the experimental determination of the high frequency velocity of sound in Li-NH$_3$ solutions and the derivation of the corresponding dielectric function using Eq 1. This provides a context to investigate the departure of the $\epsilon(Q)$ from the RPA predictions as a function of the electron density - here the r_s value has been changed between 7.4 and 10.4. These results, when complemented by literature data on liquid metals with lower values of r_s [2, 7, 8, 9, 10, 11, 12, 13, 14, 15], provide i) the r_{sth}=4.6 value as the threshold value below which the RPA properly works and ii) the characteristic dependence of the electronic dielectric function on the electron density at r_s larger than r_{sth}. These findings suggest the remarkable result that the electron density is the relevant parameter in the description of the dielectric function even when the electron response starts to be affected by complex corrections to the RPA.

The experiment was performed at the high resolution Inelastic X-rays Scattering (IXS) beamline ID16 at the European Synchrotron Radiation Facility in Grenoble (France). The measurements were carried out with a total energy resolution of ~ 1.5 meV and an exchanged

momentum, Q, resolution of 0.4 nm^{-1}. Further details of the beamline are reported elsewhere [16]. Every scan took about 210 min and the final spectra were obtained by averaging 3 to 4 scans. The Q values were selected between 1 and 15 nm^{-1}. The samples were prepared using high purity Li (nominally 99.9 %) and high purity anhydrous ammonia (nominally 99.995%). A stainless steel container, with two sapphire windows (total thickness 500 μ) and with 5 cm^3 internal volume, was kept in a cryostat at T=240.0±0.2 K. The initial solution was prepared at the limit of solubility of lithium in ammonia (20±0.5 mpm). Successive dilutions were carried out *in situ* in order to measure three other metallic concentrations: 17.5±0.5 mpm, 9.3±0.2 mpm and 6.5±0.2 mpm.

IXS spectra are reported in Fig. 1 for the solution at 17.5 mpm at a representative set of Q values. They consist of a central quasielastic line and two clear inelastic components which, as shown in Fig. 1, disperse up to Q=7 nm^{-1}. The dependence of the measured spectra on the Li concentration is shown in Fig. 2 at Q=2 nm^{-1} for the four studied solutions. The spectral line shape changes considerably on changing the Li content: the quasi-elastic line becomes more and more intense with respect to the inelastic features as the metal to insulator transition is approached (top to bottom spectra in Fig. 2). At larger Q values, particularly at the first sharp diffraction peak ($Q_M \sim 10$ nm^{-1} for the solution at 17.5 mpm, see Fig. 3b), the spectra become narrow with a width comparable to the resolution function.

The measured IXS spectra have been fitted to the convolution of the resolution function with a model function composed of a Lorentzian curve for the central line and a Damped Harmonic Oscillator (DHO) function for the inelastic signal [17]:

$$S(Q,E) = \frac{E/K_B T}{1 - e^{E/K_B T}} \left(\frac{I_c(Q)\Gamma_c(Q)}{\Gamma_c^2(Q) + E^2} + \frac{I(Q)\Gamma(Q)\Omega^2(Q)}{(\Omega^2(Q) - E^2)^2 + 4\Gamma^2(Q)E^2} \right). \quad (3)$$

The quasielastic and inelastic spectral features are defined in terms of a set of two and three parameters, respectively. Those concerning the inelastic components are related to the energy, $\hbar\Omega(Q)$, lifetime, $\Gamma(Q)$, and strength, $I(Q)$, of the acoustic-like excitations. Both Fig. 1 and Fig. 2 show that the fitting function of Eq. 3 describes well the experimental spectra. The Q-dispersions of the fitting parameter $\Omega(Q)$ are shown in Fig. 3 (left axes) together with X-ray measurements of the static structure factor, S(Q) [18] (right axes), and an indication of the location of twice the Fermi wavenumber, $2K_F$ (dotted vertical line). At low Q the acoustic excitations of the solutions show a linear dispersion (solid lines in Fig. 3) as it is expected for a sound-like mode. In the panels (a) and (b) of Fig. 3 the results for the two more metallic solutions are reported. Here, $\Omega(Q)$ shows
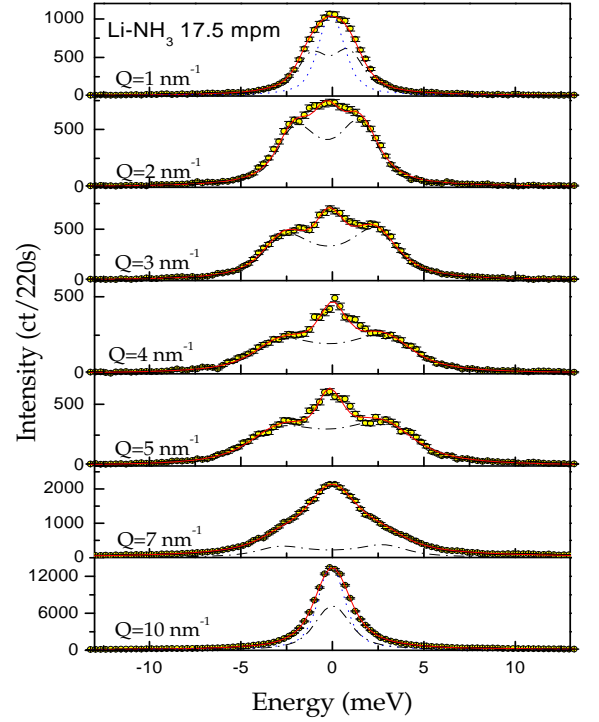

FIG. 1: Selected IXS spectra for the 17.5 mpm LiNH$_3$ solution (o) at the indicated values of the exchanged wave vector, plotted together with the total fitting function (-) corresponding to Eq. 3 and the resolution convoluted inelastic features (dot-dashed line). At Q=1 nm^{-1} and Q=10 nm^{-1} the experimental resolution function (dotted line), scaled to the maximum of the spectrum, is also reported.

a maximum between 5 and 6 nm^{-1} and then decreases reaching a minimum at a Q value close to the first maximum, Q_M, in the corresponding S(Q). This is a common finding in liquids which is usually referred to as the De Gennes narrowing [17]. A different interpretation of this minimum formulated in terms of the Q-dependence of the electronic dielectric function has instead been proposed for the 20 mpm solution [5, 19]. In fact, for Q-values of the order of K_F, Eq. 2 must be replaced by the more accurate Lindhard result [1] which has a singular point at Q = 2 K_F. This singularity would in turn induce a kink in the dispersion curve via Eq. 1. However, given the proximity of $2K_F$ to Q_M for both the 20 mpm and the 17.5 mpm solutions, it is hard to disentangle structural and electronic effects. The dispersion curves of the solutions at 9.3 mpm and 6.5 mpm reported in the panels (c) and (d) of Fig. 3 are, from this point of view, much more interesting since $2K_F$ and Q_M are here considerably different. As a matter of fact, these two dispersion curves both show a slight bending down in the proximity of the first diffraction peak (less evident for the solution at 6.5 mpm) and a small kink at Q$\sim$8 nm^{-1}, very close to 2 K_F. This kink suggests indeed the presence of a Kohn-like instability of the system at Q $\sim$ 2 K_F. This result - if
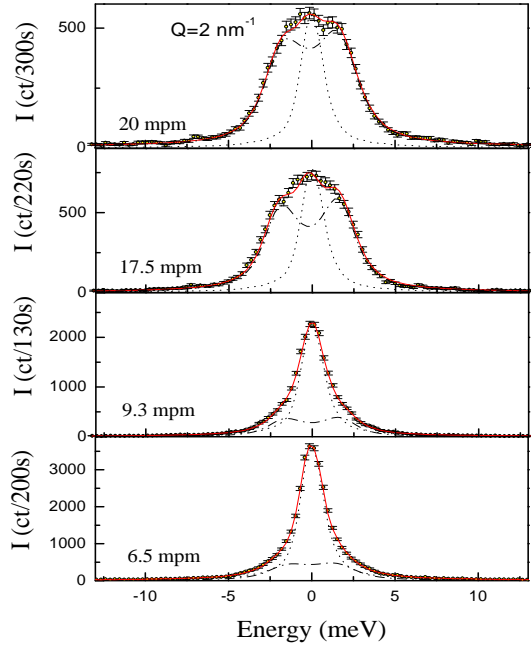
FIG. 2: Selected IXS spectra at fixed wave vector transfer Q=2 nm^{-1} for the four studied solutions. The experimental data (o) are plotted together with the experimental resolution (dotted line), the total fitting function (-) and the inelastic resolution-convoluted contributions (dot-dashed line).

FIG. 3: Dispersion curves for the acoustic excitations obtained from the fit procedure discussed in the text for the Li-NH$_3$ solutions at the indicated concentrations. The X-ray S(Q) spectra are also reported (right axes) [18]. The vertical dotted lines indicate the wave vector position corresponding to 2 K_F. The solid lines are the low Q linear fits to the dispersion curves.

confirmed with a better statistics and higher Q-resolution - would then delineate the effects of the electron-phonon coupling in these expanded liquid metals, and support the interpretation proposed earlier [5, 19]. However, these data indicate that in any case the Kohn anomaly has only a small effect on the dispersion curve, and the minimum at Q_M has mainly a structural origin.

Linear fits to the dispersion curves at low Q, reported in Fig. 3, are used to determine the high frequency sound velocity of the measured solutions: c_{Exp}(20 mpm)=1580±20 m/s, c_{Exp}(17.5 mpm)=1519±60 m/s, c_{Exp}(9.3 mpm)=1430±60 m/s and c_{Exp}(6.5 mpm)=1450±60 m/s [20]. These values are compared with the RPA expectations obtained combining Eqs. 1 and 2, i.e. $c_{RPA} = v_F \sqrt{(Zm)/(3M)}$ [1]. In this expression, knowing that the Li ions form tetrahedral complexes with the ion surrounded by four ammonia molecules [21, 22], M is identified as the mass of the Li(NH$_3$)$_4$ complex, as already proposed in refs. [5, 19]. In this picture, the solution at the limit of solubility (20 mpm) is completely made up of these complexes, while at lower Li content, the solutions can be viewed as a two component system where the Li(NH$_3$)$_4$ complexes are still stable entities embedded in the uniform background of the ammonia molecules [23]. The comparison between the c_{Exp} and c_{RPA} is presented in Fig. 4 as the ratio c_{Exp}^2 / c_{RPA}^2 as a function of r_s. The corresponding $\epsilon_{RPA}/\epsilon_{Exp}$ ratio is on the left axis. In Fig.4 we
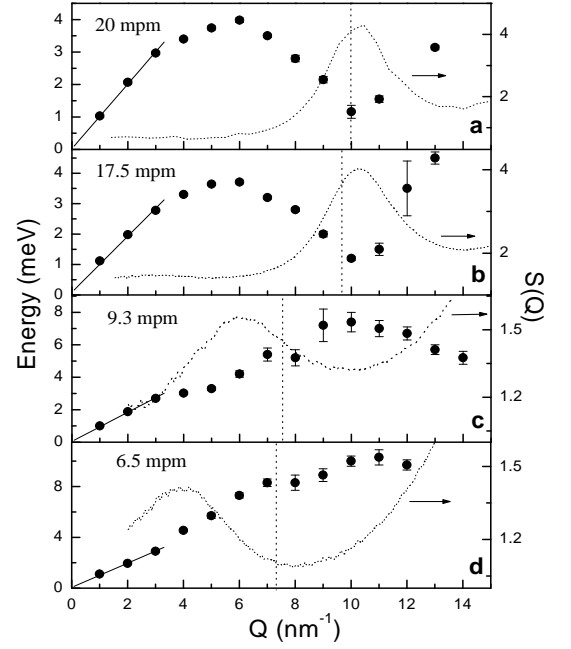
also report the results obtained for other liquid metals, as taken in the literature from ref. [13] for Al, ref. [2] for Hg, ref. [12] for Pb, ref. [11] for Li, ref. [10] for Na, ref. [14] for K, ref. [15] for Cs and ref. [8] for Rb. At low r_s, as expected, a very good agreement exists between the experimental results and the RPA predictions, confirming nicely that Eq. 1 relates the infinite frequency sound velocity and the dielectric function. A clear departure from the RPA is observed in Fig. 4 at the threshold value r_{sth}=4.6, above which c_{Exp} becomes sensibly larger than c_{RPA}.

The very intriguing result of Fig. 4 is that all the existing data follow a continuous trend despite of the very large variety of considered systems: steric effects, chemical specificities, and spatial extent of the different atoms and complexes are somehow irrelevant for c_{Exp}^2 / c_{RPA}^2 and $\epsilon_{RPA}/\epsilon_{Exp}$ - the only important parameter is r_s. In other words, regardless of a number of parameters not correctly treated by the RPA, as electronic correlations and finite ionic size effects, the electron dynamics has a general dependence on the electron density.

The results reported in Fig. 4 are further emphasized considering the r_s-dependence of the screening wave vector Q_{Exp}=Ω_{pi}/c_{Exp}, shown in the insert of Fig. 4. Here, Q_{Exp} is compared with Q_{RPA} and with the SSTL theoretical prediction [24], which is an attempt to extend the range of the RPA by introducing a local field correction
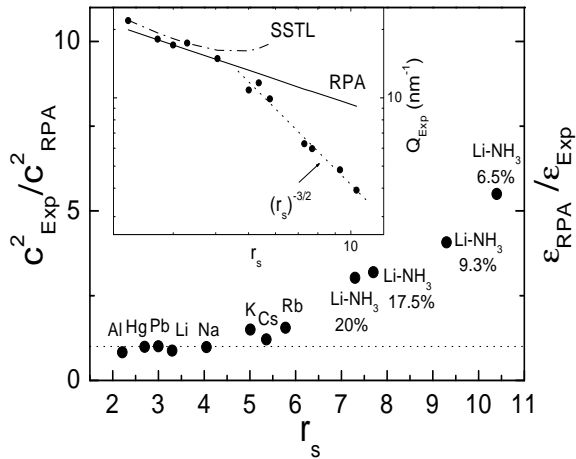
FIG. 4: Ratio between the experimental and the RPA squared sound velocities (left axis) as a function of r_s for different liquid metals [2, 8, 10, 11, 12, 13, 14, 15]. These data correspond via Eq.1 to the ratio between the RPA and the experimental dielectric function (right axis). The dotted line corresponds to the unity value. In the insert the corresponding experimental screening wave vectors (closed circles) are compared to the RPA (solid line) and to the SSLT theory (dot dashed line). The dotted line emphasizes the phenomenological $r_s^{-3/2}$ law obeyed by metals for $r_s \geq 4.6$.

readjusted to an external field. Once more, experiment and theories are in good agreement up to r_{sth}, while a clear deviation is observable above r_{sth}. We also note that the SSLT theory not only does not improve RPA in describing Q_{Exp}, but seems to predict a departure from RPA opposite to the one experimentally measured. Finally, it is very interesting to note that for $r_s \geq r_{sth}$, Q_{Exp} is extremely well reproduced by an empirical $r_s^{-3/2}$ dependence.

In conclusion, we presented IXS measurements in expanded liquid metals with high r_s allowing the determination of the high frequency sound velocity: these data, along with literature data for metals with lower r_s, emphasize the breakdown of existing electron gas theories above a threshold value r_{sth}. Most interestingly, the dielectric function, when the electron-electron correlations become increasingly important, shows a departure from RPA that follows a characteristic behavior which depends only on the electron density and not on the specific details of the considered systems. Future theories on the electronic dynamics must be compared with such a finding in order to test their ability to describe the deviations from the RPA.

[1] N. W. Ashcroft and N. D. Mermin, *Solid State Physics* (W. B. Saunders Company, 1976).
[2] L. E. Bove, F. Sacchetti, C. Petrillo, B. Dorner, F. Formisano, and F. Barocchi, Phys. Rev. Lett. **87**, 215504 (2001).
[3] C. A. Burns, P. Abbamonte, E. D. Isaacs, and P. M. Platzman, Phys. Rev. Lett. **83**, 2390 (1999).
[4] C. A. Burns, P. Giura, A. Said, A. Shukla, G. Vankò, M. Tuel-Benckendorf, E. D. Isaacs, and P. M. Platzman, Phys. Rev. Lett. **89**, 236404 (2002).
[5] F. Sacchetti, E. Guarini, C. Petrillo, L. E. Bove, B. Dorner, F. Demmel, and F. Barocchi, Phys. Rev. B **67**, 014207 (2003).
[6] L. E. Bove, B. Dorner, C. Petrillo, F. Sacchetti, and J. B. Suck, Phys. Rev. B **68**, 024208 (2003).
[7] J. R. D. Copley and J. M. Rowe, Phys. Rev. A **9**, 1656 (1974).
[8] J. R. D. Copley and J. M. Rowe, Phys. Rev. Lett. **32**, 49 (1974).
[9] L. E. Bove, F. Sacchetti, C. Petrillo, and B. Dorner, Phys. Rev. Lett. **85**, 5352 (2000).
[10] T. Scopigno, U. Balucani, G. Ruocco, and F. Sette, Phys. Rev. E **65**, 031205 (2002).
[11] T. Scopigno, U. Balucani, A. Cunsolo, C. Masciovecchio, G. Ruocco, F. Sette, and R. Verbeni, Europhys. Lett. **50**, 189 (2000).
[12] O. Soderstrom, J. R. D. Copley, J.-B. Suck, and B. Dorner, J. Phys. F **10**, L151 (1980).
[13] T. Scopigno, U. Balucani, G. Ruocco, and F. Sette, Phys. Rev. E **63**, 011210 (2000).
[14] C. Cabrillo, F. J. Bermejo, M. Alvarez, P. Verkerk, A. Maira-Vidal, S. M. Bennington, and D. Martìn, Phys. Rev. Lett. **89**, 075508 (2002).
[15] T. Bodensteiner, C. Morkel, W. Gläser, and B. Dorner, Phys. Rev. A **45**, 5709 (1992).
[16] C. Masciovecchio, U. Bergmann, M. Krisch, G. Ruocco, F. Sette, and R. Verbeni, Nucl. Instrum. Methods Phys. Res. **Sect B 111**, 181 (1996).
[17] U. Balucani and M. Zoppi, *Dynamics of the Liquid State* (Clarendon press Oxford, 1994).
[18] P. Giura, R. Angelini, M. Dimichiel, and C. Burns, to be published.
[19] C. A. Burns, P. M. Platzman, H. Sinn, A. Alatas, and E. E. Alp, Phys. Rev. Lett. **86**, 2357 (2001).
[20] These values of c_{Exp} are larger than the ultrasonic ones reported by Bowen et al. Phys. Rev. 168, 114 (1968). This has to be expected since, in these systems, the ultrasound technique probes the speed of sound in the viscous regime, as opposed to the elastic regime probed by inelastic X-ray and neutron scattering.
[21] J. C. Wasse, S. Hayama, N. T. Skipper, C. J. Benmore, and A. K. Soper, J. Chem. Phys. **111**, 2028 (1999).
[22] J. C. Wasse, S. Hayama, N. T. Skipper, and H. E. Fischer, Phys. Rev. B **61**, 11993 (2000).
[23] D. N. Knapp and H. D. Bale, J. Appl. Crystallogr. **11**, 606 (1978).
[24] K. S. Singwi, A. Sjölander, M. P. Tosi, and R. H. Land, Phys. Rev. B **1**, 1044 (1970).